Aerosol Science and Technology

ISSN: 0278-6826 (Print) 1521-7388 (Online) Journal homepage: www.tandfonline.com/journals/uast20

Characterization of airborne tire particle emissions under realistic conditions on the chassis dynamometer, on the test track, and on the road

Linda Bondorf, Manuel Löber, Tobias Grein, Lennart Köhler, Fabius Epple, Tobias Schripp, Manfred Aigner & Franz Philipps

To cite this article: Linda Bondorf, Manuel Löber, Tobias Grein, Lennart Köhler, Fabius Epple, Tobias Schripp, Manfred Aigner & Franz Philipps (2025) Characterization of airborne tire particle emissions under realistic conditions on the chassis dynamometer, on the test track, and on the road, Aerosol Science and Technology, 59:5, 623-634, DOI: 10.1080/02786826.2025.2464215

To link to this article: https://doi.org/10.1080/02786826.2025.2464215

AEROSOL SCIENCE AND TECHNOLOGY
2025, VOL. 59, NO. 5, 623–634
https://doi.org/10.1080/02786826.2025.2464215

Characterization of airborne tire particle emissions under realistic conditions on the chassis dynamometer, on the test track, and on the road

Linda Bondorf[a]*, Manuel Löber[a]*, Tobias Grein[a], Lennart Köhler[b], Fabius Epple[b], Tobias Schripp[a]**, Manfred Aigner[a], and Franz Philipps[b]

[a]German Aerospace Center (DLR), Institute of Combustion Technology, Stuttgart, Germany; [b]German Aerospace Center (DLR), Institute of Vehicle Concepts, Stuttgart, Germany

ABSTRACT

Tires have already been identified as a major source of microplastics and airborne particles, and with the increasing use of alternative powertrains and heavier vehicles, the importance of tire and road wear particles (TRWP) is growing. As part of this comprehensive study, a new sampling system was developed to measure the particle number concentration (PNC) of TRWP emissions from 4 nm to 10 µm. Airborne emissions were characterized on the chassis dynamometer using an aerosol fast sizer, which revealed a bimodal size distribution with a dominant ultrafine emission mode at approximately 10 nm and a larger mode at 270 nm. Investigation of the collected particles using scanning electron microscopy (SEM) and energy dispersive X-ray spectroscopy (EDS) provided insight into two different formation mechanisms for ultrafine particles including evaporation and condensation. The emission indices of four driving cycles (WLTC Class 3, LA4, US06, and Großglockner) were determined on the chassis dynamometer and compared with a real driving emission test. The influence of road surface and lateral acceleration on the amount of TRWP and their size distribution was investigated by mobile measurements on the test track and on the real road. Both the choice of test cycle and the test environment have a significant influence on detected tire emissions: The number of particles emitted per kilometer differs strongly between the driving cycles, while the test environment and cornering have an influence on the particle size distribution.

GRAPHICAL ABSTRACT

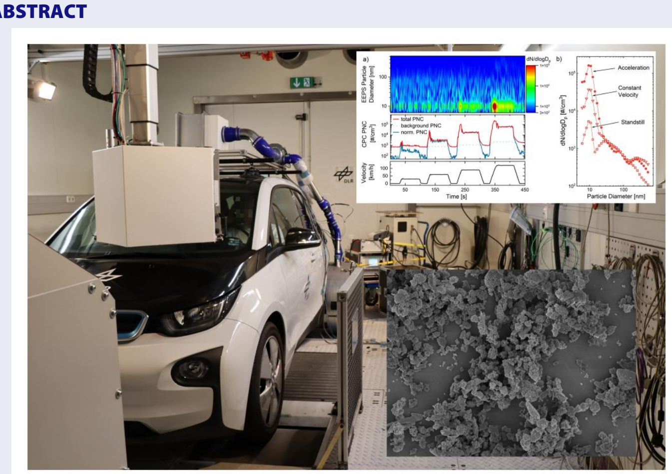

ARTICLE HISTORY
Received 12 August 2024
Accepted 21 January 2025

EDITOR
Jason Olfert

CONTACT Linda Bondorf linda.bondorf@dlr.de German Aerospace Center (DLR), Institute of Combustion Technology, Stuttgart 70569, Germany.
*Joint first authors. Both authors contributed equally.
**Current affiliation: Center for Aviation, Zurich University for Applied Sciences (ZHAW), Winterthur, Switzerland

Supplemental data for this article can be accessed online at https://doi.org/10.1080/02786826.2025.2464215.

1. Introduction

Due to the ongoing electrification of road traffic, non-exhaust emissions such as brake and tire wear and road particle resuspension will account for a large proportion of urban particulate matter pollution in the future (Lin et al. 2022; Jandacka and Durcanska 2019). For brakes, the regulation of emissions based on laboratory measurements has already been implemented in the Euro 7 standards (UN 2023; EU 2024). In addition, work is currently underway on a variety of methods to reduce emissions from braking systems, including coating brake disks (Aranke et al. 2019) or filtering brake dust (Hascoët and Adamczak 2020). Reducing tire and road wear particles (TRWP) is more complex because the contact area between the tire and the road is an open system and the emission depends on numerous parameters. Critical research gaps include the determination of tire emission factors, the study of surface-tire interaction, the influence of weather and driving behavior as well as the development of standardized measurement methods (Gehrke et al. 2023; Dalmau et al. 2020).

The evaluation of tire wear and the comparison of different tire types is primarily based on the total mass loss of the tire in grams per kilometer driven, which is an important parameter for estimating macro- (5 – 25 mm) and microplastic (< 5 mm) emissions from tires (Charbouillot et al. 2023; GRBP-78-17 2023). However, to determine the full impact of TRWP on air quality, airborne particle mass (PM10, PM2.5) should be accompanied by information on particle size (PSD) and particle number (PN). Whereas wear particles are typically dominated by abrasion particles, studies of airborne tire wear emissions show particle diameters ranging from 10 to 300 nm (Kumar et al. 2013; Dahl et al. 2006; Park, Kim, and Lee 2018), with a high proportion of particles between 15 and 50 nm (Fussell et al. 2022). Ultrafine particles (UFP, $d < 100$ nm) are particularly hazardous because they occur in high numbers compared to larger airborne particles, and their high surface-to-volume ratio results in high chemical reactivity (Schraufnagel 2020). As the chemical nature of the particles is still being investigated (Johannessen et al. 2022), a toxicological assessment is rather difficult. Particles in exhaust gas of comparable size are known to penetrate the human body, entering the circulatory system and cellular organelles (Kwon, Ryu, and Carlsten 2020).

Component tests, such as road simulators (G. Kim and Lee 2018; Grigoratos et al. 2018; Schläfle, Unrau, and Gauterin 2023; Dahl et al. 2006), or customized dynamometer test rigs (Chang et al. 2020; Tonegawa and Sasaki 2021), are used to generate and study the release of airborne tire wear particles, allowing a systematic investigation of various relevant parameters, such as ambient temperature, vehicle weight, and tire properties. However, real-world conditions, such as the interaction between the tire and the road surface or the driving behavior of the vehicle, cannot be comprehensively represented by those systems. For this purpose, test vehicles are chosen as they allow airborne particle sampling while driving on a chassis dynamometer (Li et al. 2023), test track (Mathissen et al. 2011; Beji et al. 2021) or on the road (Lee et al. 2013; Feißel et al. 2024; Beji et al. 2021). Previous studies have used a range of different test vehicle setups, from particle collection through a tube or line near the wheel (Li et al. 2023; Lee et al. 2013; Mathissen et al. 2011; Kwak et al. 2013; Beji et al. 2021) to more complex systems including a brake capsule (Feißel et al. 2024).

Testing a particle collector for tire particles under laboratory and real-life conditions requires a great deal of technical effort in order to mimic the relevant properties. In addition, mobile measurements usually require the use of non-laboratory test equipment due to power and space constraints. However, these may not allow a complete characterization and identification of tire wear particles.

This study presents a novel on-vehicle sampling setup using two separate ventilated brakes (Bondorf et al. 2023) and tire housings to quantify and characterize airborne tire emissions from a battery electric test vehicle under realistic conditions. Online particle measurements between 4 nm and 10 µm are performed on a dynamometer, on a test site and on the road. In addition, particles are collected for morphological and chemical analysis using scanning electron microscopy (SEM) and energy dispersive X-ray spectroscopy (EDS). The investigations aim to determine the influence of test conditions (test environment and test cycles) on the TRWP. In addition to the quantification of emissions, the characterization of size distribution and morphology will provide the basis for a better understanding of the particle formation processes and the interaction between tire and roller or road surface to develop future methodology for tire emission testing.

2. Materials and methods

2.1. Experimental setup

2.1.1. Particle generation

A regular battery electric car, a BMW i3, was selected and modified for this experiment. First registered in

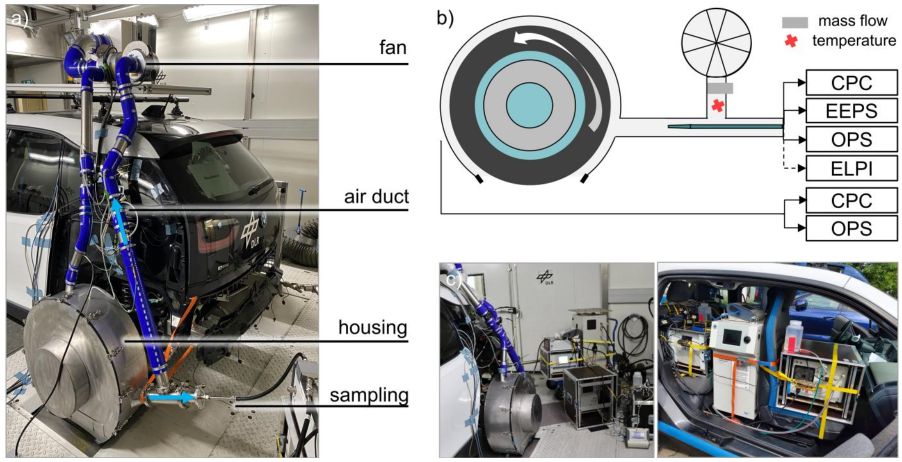

Figure 1. (a) Test setup on the vehicle with a tire enclosure and ventilation system. (b) Schematic representation of the measurement setup, including isokinetic sampling and instrumentation. (c) Spatial integration of the measurement equipment during tests on the chassis dynamometer (left) and for mobile measurements (right).

2015, it had a vehicle weight of 1228 kg and a battery capacity of 60 Ah. The test vehicle was designed to independently measure brake particle and TRWP emission on-board. The particulate sampling setup was installed on the left side of the vehicle's rear axle. The tested wheel is driven, not steered, and contains a disk brake. Brake results, measured in the described test setup, are already published (Bondorf et al. 2023). New tires from the same batch as the standard tires of the reference vehicle (Bridgestone Ecopia EP 500, 155/70 R 19 84 Q) were used in for the chassis dynamometer tests and the mobile measurements respectively.

2.1.2. Particle collection

Figures 1a and b show the test setup for the tire emission study. It includes the tire casing, filtered air ventilation, sampling probe, and multiple sensors. A spacer plate separates the tire from the brake, allowing each to be tested separately. The brake is a closed system, while the tire casing is open to the road. A measuring rim (WTT Dx, imc Test & Measurement GmbH) on the left rear wheel measures its torque and velocity. In addition, a GPS module (Racelogic RLVBSS05) records vehicle velocity, slope and acceleration during mobile measurements.

Preliminary tests showed that the use of more than one fan (one before the particle generation point, one after the particle generation point) was not beneficial to a controlled, steady TRWP measurement. Therefore, the air inlet was closed and the system was operated with a single adjustable fan at the outlet drawing air through the main tube. The negative pressure of the fan draws air through the outlet at a flow rate of 130 m^3/h. Integrated sensors monitor the air mass flow and temperature of the ventilation system (Bosch HFM 5, Type K, AMS 4712-1200-B).

Figure 1a shows an isokinetic in-line sampling of the aerosol sample integrated into the duct behind the outlet. The diameter of the sampling nozzle is matched to the airflow in the system. Flow dividers and carbonized tubing carry the collected air sample to the particle analyzers inside of the car. Losses within the sampling system were determined prior to the experiment by salt (NaCl) particles generated by a portable test aerosol generator (Model 3073, TSI) and comparison of the inlet and outlet particle number concentration and particle size distribution. The corresponding particle loss curve is shown in the online supplementary information.

Since TRWP sampling occurs in an open system, the sample air contains both tire particulate emissions and particles already present in the ambient air. Therefore, background monitoring is required to quantify TRWP emissions. The background concentration is sampled through a carbonized tube outside the tire casing 4 cm above the ground. Net particle number concentrations are calculated by subtracting the background concentration from the total particle concentrations (main sample) at the outlet of the tire casing.

2.1.3. Particle analysis

The instruments for measuring particle number concentration (PNC) and particle size distribution (PSD) were selected due to their high time resolution (1 Hz) and high response time. The selected combination of particle measurement instruments covers a particle size range from 4 nm to 10 µm. Two Condensation Particle Counters (CPC, TSI 3752/TSI 3776) quantify

Table 1. Overview of the test cycles used in this study including the test environment, time, distance, and average velocity.

Test Cycle	Test Environment	Time [s]	Distance [km]	Avg. Velocity [km/h]	Figure No.
ZEDU Accelerate	chassis dynamometer	390	8.12	75	2
WLTC Class 3b	chassis dynamometer	1800	23.2	46.5	4
LA4	chassis dynamometer	1369	12.07	31.5	4
US06	chassis dynamometer	596	12.8	77.9	4
Großglockner	chassis dynamometer	1904	21.1	40	4
ZEDU A&B	test track, chassis dynamometer	1115	7.04	22.7	5, 6
ZEDU Cornering	test track	227	0.96	15.2	7
ZEDU RDE	on-road, chassis dynamometer	3619	47.4	47.2	8

PNC for diameters between 4 nm/2.5 nm and 3 µm. An Engine Exhaust Particle Sizer (EEPS, TSI Model 3090) measures PSD between 5.6 and 560 nm in 32 channels. It should be noted that the EEPS is designed for high PNC. Therefore, the noise is increased at concentrations below 8×10^3 #/cm^3. For this reason, the CPCs were used as a quantification basis while the EEPS delivers information on the size of the observed particles. Fine and coarse particles from 300 nm to 10 µm are detected by two Optical Particle Sizers (OPS, TSI Model 3330), which measures size-selective in 16 channels.

Additional sampling with a low-pressure cascade impactor (ELPI+, DEKATI) allows a size-selective collection of particles with an aerodynamic diameter between 15 nm and 10 µm on 14 sampling stages with a sampling flow of 10 l/min. Particle collection is performed without voltage in the charger or electrodes. Particle deposition on aluminum and polycarbonate substrates is analyzed using scanning electron microscopy (Ultra Plus, Carl Zeiss). The elemental composition of the particles is determined by an attached EDX detector (UltimMax 65 mm^2, Oxford Instruments). Stationary tests on the dynamometer are performed with the measurement equipment outside the vehicle, while for mobile measurements the instruments are integrated into the car, as shown in Figure 1c. In the latter case, the instrumentation is powered by a 12.8 V battery (Victron Energy) with a 230 V inverter independent of the vehicle's electrical system.

2.2. Test environment and conditions

The TRWP emissions were investigated in three test scenarios: on a chassis dynamometer, on a test track, and under real-road driving conditions.

The chassis dynamometer tests were conducted at the DLR Institute of Vehicle Concepts in Stuttgart, Germany, using four independently driven 48-inch rollers with a maximum continuous power of 100 kW each. The roller coating material consists of a CrNiMo adhesive layer and a top layer of FeCrB with a technical roughness of Rz 114. In addition, the chassis dynamometer is equipped with an air conditioning and ventilation system with integrated air filtration. A background particle concentration of approx. $1*10^3$ #/cm^3 can be achieved within the test cell.

A traffic training area in Asberg (Germany) was selected as the test track for the mobile measurements. The area was rented exclusively, with no other vehicles on the track. On this test track, the vehicle velocity is limited to 75 km/h due to space constraints. Real Driving Emissions (RDE) measurements were conducted on a 47.4 km route in and around Stuttgart, Germany, including urban, rural and motorway sections, as described in Bondorf et al. (2023). The test drives were conducted in the morning and afternoon outside of peak traffic hours to avoid heavy traffic and traffic jams.

TRWP emissions are measured and characterized using in-house developed test cycles such as ZEDU[1] Accelerate, as well as test cycles derived from driving data on the test track (ZEDU A&B and ZEDU Cornering) or on the road (ZEDU RDE). In addition, the four standardized driving cycles WLTC Class 3b, LA4, US06 and Großglockner are used. Table 1 provides an overview of the test cycles used in the three different test environments and their key parameters time, distance, and average velocity.

3. Results and discussion

3.1. Chassis dynamometer

The described setup was first operated on the chassis dynamometer, where the low background concentrations allow a precise and reproducible investigation of even low tire wear emissions.

3.1.1. Normalization and particle size distribution

TRWP emissions were characterized using the short "ZEDU Accelerate" test cycle shown in Figure 2a.

[1]ZEDU is the abbreviation for the project name "Zero Emission Drive Unite Generation 1", within the framework of which the test cycles were defined.

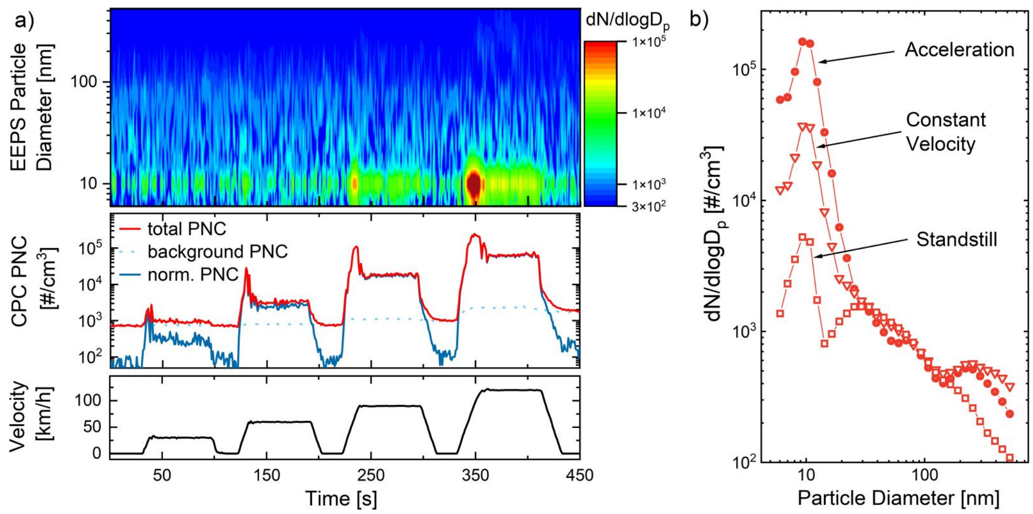

Figure 2. (a) TRWP emissions during acceleration, constant velocity and braking on the chassis dynamometer: Total, background and normalized PNC of fine particles from CPC measurements, as well as the total EEPS particle size distribution. (b) PSD for standstill, constant velocity and acceleration during the last section of the driving cycle (second 320–450) measured by the EEPS.

From bottom to top, the vehicle velocity, the particle number concentration measured by CPCs, and the particle size distribution measured with an EEPS are displayed. The normalized particle concentration for each OPS and CPC is calculated by subtracting the background concentration outside the tire enclosure from the PNC measured at the primary sampling location inside the tire enclosure at 1 Hz.

The PNC is displayed by the total concentration (red), the background concentration (light blue), and the difference of both, called normalized concentration (dark blue). The background concentration is only significant at low velocities as emphasized by the normalized PNC. At 30 km/h the background contribution to the total emissions is around 20%, being only a few percent at 60 km/h and less than 1% above 90 km/h, as visible in Figure 2a.

As shown in the normalized CPC data, tire particles are predominantly generated during vehicle acceleration, but are also emitted at constant velocity. For the latter, the average concentration increases exponentially with 422 #/cm^3 at 30 km/h, 2242 #/cm^3 at 60 km/h, 16004 #/cm^3 at 90 km/h, and 60029 #/cm^3 at the maximum velocity of 120 km/h. This trend is also visible in the EEPS measurements, revealing that most of the particles emitted during acceleration or constant velocity driving are in the 10 nm range.

A more detailed analysis of the PSD is shown in Figure 2b, where the average size distribution measured with the EEPS for halt, acceleration and constant velocity is plotted. Note that the size distribution has not been normalized by a background measurement. However, the standstill phase can be used as a reference where the emissions are in the range of 10^3 #/cm^3 with two modes being visible around 10 and 30 nm. During acceleration, the 10 nm mode increases by two orders of magnitude while the 30 nm particles remain constant. An additional mode becomes visible in the fine particle range with a maximum of 270 nm. At constant velocity, both the 10 nm and 270 nm emissions also increase, with lower UFP emissions than at acceleration, but higher fine particulate emissions. Based on the differences between the size distribution at halt and while driving, it can be concluded that ultrafine particles with a diameter of about 10 nm as well as fine tire particles at 270 nm are emitted.

Tire particulate emissions in the UFP range are in good agreement with several road simulator tests (Kim and Lee 2018; Grigoratos et al. 2018; Dahl et al. 2006; Foitzik et al. 2018). In the study by Foitzik et al. an EEPS was used for the size determination, similar to this present study, and a dominant emission mode was also observed at 10.8 nm (Foitzik et al. 2018). Fine emissions between 100 and 300 nm have also been detected in other emission tests (Alves et al. 2020; Beji et al. 2021). However, these were not reported in the EEPS measurements, on the road simulator (Foitzik et al. 2018), or on the road (Mathissen et al. 2011).

3.1.2. Morphological and chemical analysis

In order to get insights into particle morphology and chemical composition, particles were collected on the chassis dynamometer using a low-pressure impactor

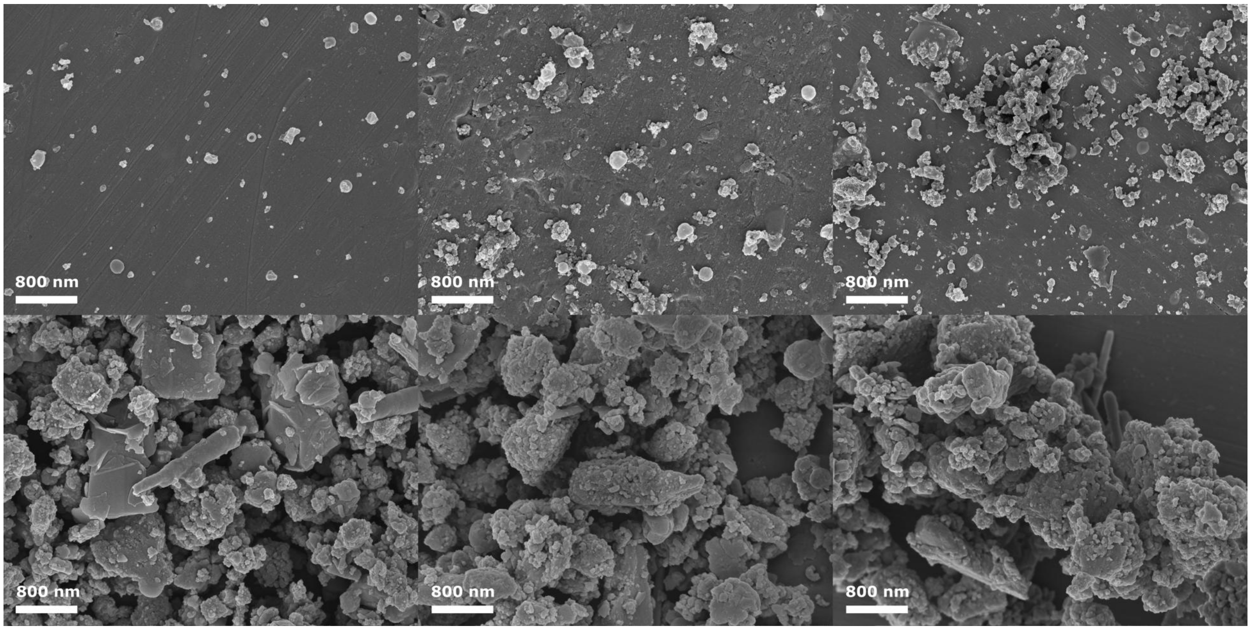

Figure 3. Micrograph of particles collected with a cascade impactor during measurements on the chassis dynamometer. The ELPI stages 2, 4, 5 (upper row from left), 7, 8 and 10 (lower row from left) are depicted. The images were taken at a magnification of 20 kx and an EHT of 3 kV. In addition, the samples were coated with a 10 nm thick layer of platinum.

and were investigated by SEM and EDS. In Figure 3 micrographs of six different impactor stages[2] are shown, on which different types of particles are visible. In stage 2, particles from around 20 nm to 200 nm in diameter are present, and two different types of particle morphology can be described. Both types have soft edges with one type almost spherical and the second one more irregularly shaped. The spherical particles are mentioned in the literature as well, where an origin from carbon black or ZnO/ZnS inclusions is assumed (Dahl et al. 2006). However, mainly carbon is detected with EDS at those particles. Since the small particles are presumed to be volatile, the spherical particles likely consist of volatile organic compounds that are later condensed to solid spherules. Uncoated samples showed rapid degradation of these spherical particles when irradiated with the electron beam, indicating their volatile nature. In stage 4 similar particle shapes can be observed, with slightly larger spherical ones around 50 to 300 nm in diameter and irregular agglomerated shapes. Stage 5 includes particles between 100 and 600 nm in diameter. Apart from the aforementioned spherical particles, larger shapes consisting of smaller grains that appear to be fused, are visible. In addition, a third type of particle with an elongated, cigar-shaped form appears. The same particle shape can be seen in stage 7, where they are somewhat larger. Similar elongated particles have already been described in the literature (Park, Kim, and Lee 2018) and can be attributed to tire wear produced mechanically by the rolling up of several thin layers. EDS spectra show C, Fe and O as main elements, of which C originates from the tire tread and iron (probably oxidized) from the surface of the dynamometer drum.

Besides these elongated shapes, two more platelet-like morphologies appear. The first of those (visible on the left edge of the cigar-shaped particle) has a smooth surface and seems to consist of different layers. The second type (visible below the cigar-shaped particle) is characterized by a slightly rougher surface with some grooves that look like grinding marks. In stage 8 similar particle shapes can be observed, with the elongated shape as long as 5 µm (not visible at the high magnification depicted in Figure 3). The irregularly shaped, most abundant particles are rich in Fe, which originated from the dynamometers drum surface. Furthermore, platelet-shaped particles are rich in tungsten, an element that hints to the presence of brake wear particles (as a coated disk was used during the same campaign). In stage 10 the particle size varies from roughly 500 nm to several µm in diameter, with the predominant particle shape being platelet shaped and encrusted by smaller grains.

[2]The aerodynamic diameters, at which 50% of the incoming particles are collected at each stage (called D50), as determined by the manufacturer's calibration, are 16 nm, 54 nm, 94 nm, 250 nm, 380 nm and 940 nm for the respective stages 2, 4, 5, 7, 8 and 10.

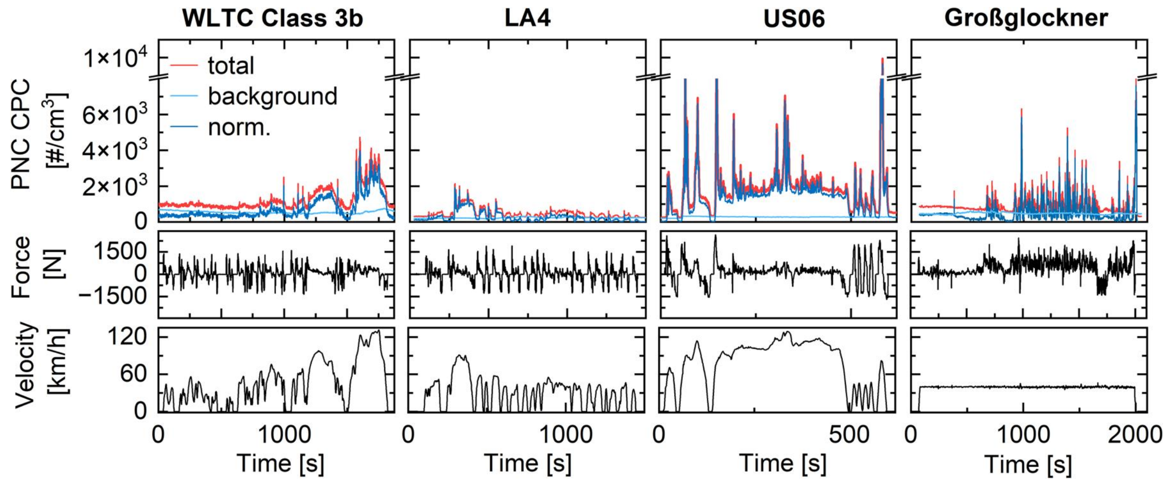

Figure 4. Velocity profile, wheel force and PNC measured by the CPC for the four driving cycles WLTC Class 3b, LA4, US06 and Großglockner. For PNC, the total concentration at the main sampling point, the background concentration before the enclosure, and the difference between the two is the normalized PNC.

Table 2. Particulate emission indices for particles between 4 nm and 3 µm in diameter (CPC) emitted from the left rear tire of the test vehicle.

Driving Cycle	Avg. Velocity [km/h]	Avg. Force [N]	(Ultra-)fine particle emission index of the left rear tire [#/km]	EI / EI_{RDE}
ZEDU RDE	47.2	316.6	1.72×10^9	1
WLTC Class 3b	46.5	277.7	2.13×10^9	1.24
LA4	31.5	235.9	1.15×10^9	0.67
US06	77.9	487.1	2.75×10^9	1.60
Großglockner	40.0	505.1	1.79×10^9	1.04

3.1.3. Driving cycles and emission indices

Four different driving cycles were measured on the dynamometer, which were developed for the determination of combustion emissions and are commonly used. WLTC Class 3b, LA4, and US06 involve a velocity change without a gradient, while the Grossglockner cycle represents a gradient profile with a constant velocity. In addition, the ZEDU RDE, which is self-defined from a real drive, was tested and is plotted in Figure 8.

Figure 4 shows the vehicle velocity and force on the wheel measured by the dynamometer for the four standard cycles. For the PNC measured by the CPC, the total (red), the background (light blue), and the normalized (dark blue) are depicted.

The emission indices (EI) for the left rear tire can be calculated as the sum of the product of the normalized particulate emissions and the known total volume flow for the entire driving cycle by Equation (1)

$$EI = \sum_{t_{start}}^{t_{end}} \left(PNC_{norm.} \left[\frac{\times s}{cm^3} \right] \times V_{total} \left[\frac{cm^3}{s} \right] \right) \quad (1)$$

All emission indices are in the range of 10^6 # as shown in Table 2. The LA4 has the lowest value at 1.15×10^9 #/km, which is expected, as it also has the lowest average velocity and average force on the wheel. This is followed by the ZEDU RDE with 1.72×10^9 #/km, the Grossglockner with 1.79×10^9 #/km and the WLTC Class 3 with 2.13×10^9 #/km. The US06, which has the highest average velocity, has the highest emissions per kilometer with 2.75×10^9 #/km. Although the relationship between average velocity and the level of particulate emissions is linear to a first approximation, the WLTC Class 3 produces significantly higher emissions than the RDE, despite its lower average velocity and average power. A comparison of the driving cycles designed to measure combustion emissions with our RDE shows that only LA4 underestimates TRWP emissions. For the other three driving cycles, they are above the RDE.

3.2. Mobile measurements

In order to measure emissions on a real road surface and with lateral acceleration, the on-vehicle test setup was used on a test track and on the road. Vehicle velocity, acceleration and gradient were determined during the tests, which were then repeated on the chassis dynamometer, allowing a direct comparison of both test environments.

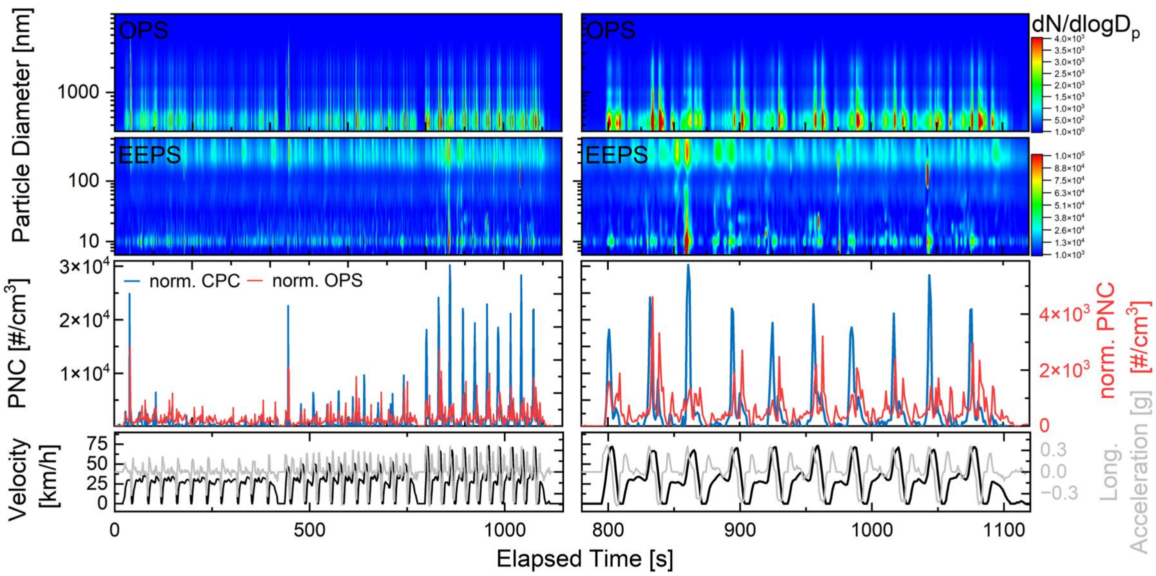

Figure 5. (a) Comparison of normalized particle emissions on the test track (blue) and on the chassis dynamometer (red) during acceleration and braking measured by the CPC. (b) Particle size distribution for both test environments measured by the EEPS. The total PSD is an average over the test cycle including acceleration, braking and standstill (elapsed time between 780 and 1097 s).

3.2.1. Acceleration and braking

The emissions for ten consecutive acceleration and braking events conducted on the test track at 30 km/h, 50 km/h, and 70 km/h are shown in Figure 5 (left-hand side). A more detailed view of the tests at 70 km/h is shown on the right-hand side. Vehicle velocity and longitudinal acceleration are displayed at the bottom of the graph, in black and grey respectively. As can be observed in the velocity data, acceleration and deceleration occur in immediate succession.

Compared to the chassis dynamometer, the environmental background concentration is higher and more variable, nevertheless, normalization has been applied to the following results to determine TRWP emissions. The normalized particle number concentration is represented in blue for ultrafine to fine particles (CPC) and in red for fine to coarse particles (OPS). As a general trend, it can be observed that the peak concentrations increase with increasing velocity in both size ranges on the left part of the figure. Despite the same environmental conditions and similar velocity curves, the emission peaks vary considerably between the ten replicates, especially during the first two velocities.

Exceptionally high emissions occur at the beginning of each measurement segment after a short standstill period (40 s, 447 s). However, the size distribution of the OPS shows that these are larger particles than those detected during the test. This could indicate the resuspension of deposited particles on the tires, the road or in the sampling system, that are released during the first acceleration. A more detailed representation of the emissions in the 70 km/h test range (right-hand side) shows that the emission peaks have two maxima. This indicates that they consist of two superimposed emission events, which are acceleration and braking.

In the contour diagrams for EEPS and OPS the size of the particulate emissions can be assigned, whereby it should be noted that the size distribution also contains the background concentration at the test location. There are two emission modes in the ultrafine range at 10 nm and about 60 nm. In addition, a third mode in the fine particulate range is recorded by the EEPS with a maximum diameter at 270 nm. The fine particle mode is also recorded by the OPS measurements, where most emissions are visible at the lower detection limit between 300 and 450 nm. Therefore, most particles recorded by the OPS are also detected by the CPC, since they are within its size range of 4 nm–3 µm.

A similar acceleration/brake test, based on the velocity profile and the recorded brake pressure, was conducted on the chassis dynamometer. The direct comparison of the measurement results is shown in Figure 5a, with the dynamometer values in red and the test site values in blue.

In both test environments, the peak height varies greatly from event to event. In the case of the chassis dynamometer, it ranges from 1.1×10^4 to 4.2×10^4, which is on average 19% higher than the peak height measured on the test track. Considering the total

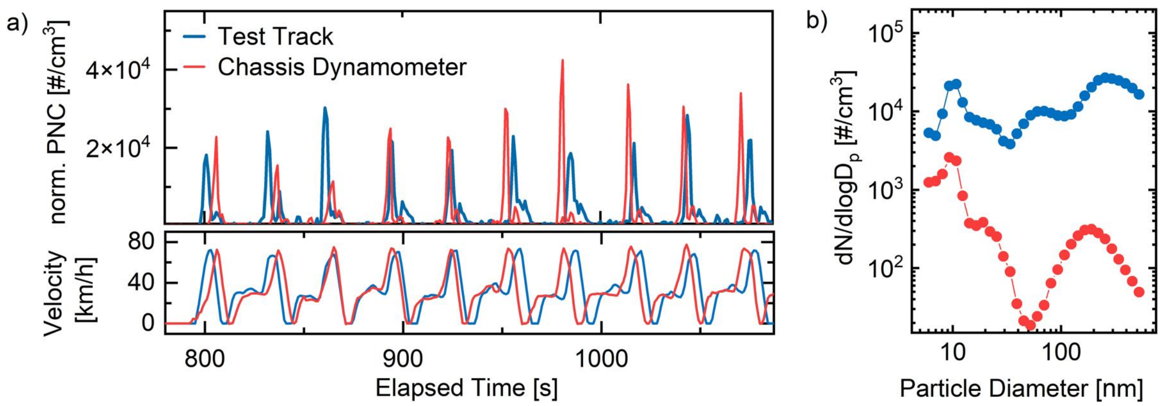

Figure 6. (a) Particle emissions during cornering on the test track: Total particle number concentration of (ultra) fine particles and the total particle size distribution, both measured by EEPS. (b) Comparison of the total particle size distribution for cornering (170 s–210 s) and acceleration and braking (Figure 7, 750 s–1150 s).

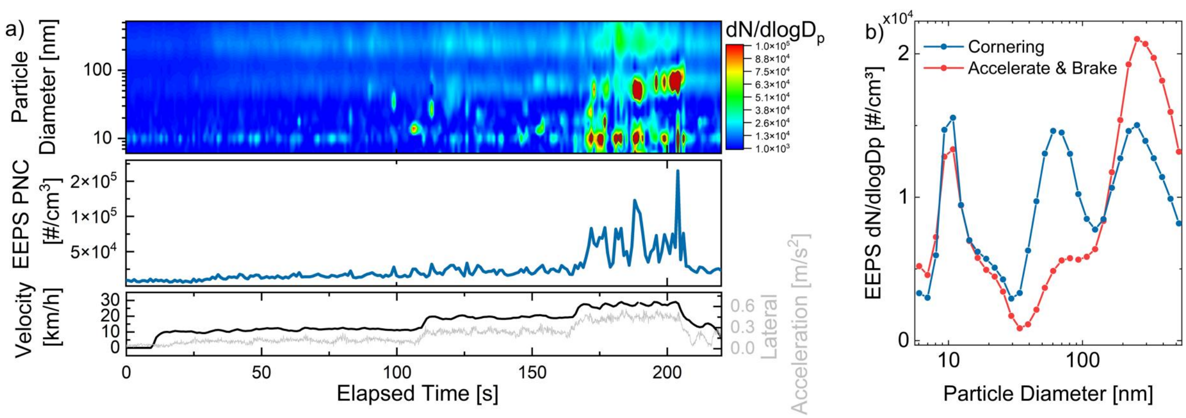

Figure 7. TRWP emissions during acceleration and braking on the test track: Normalized particle number concentration of coarse and fine particles as well as the total particle size distribution, measured by EEPS and OPS. An overview of the test drive is shown on the left, an enlargement of the last section on the right.

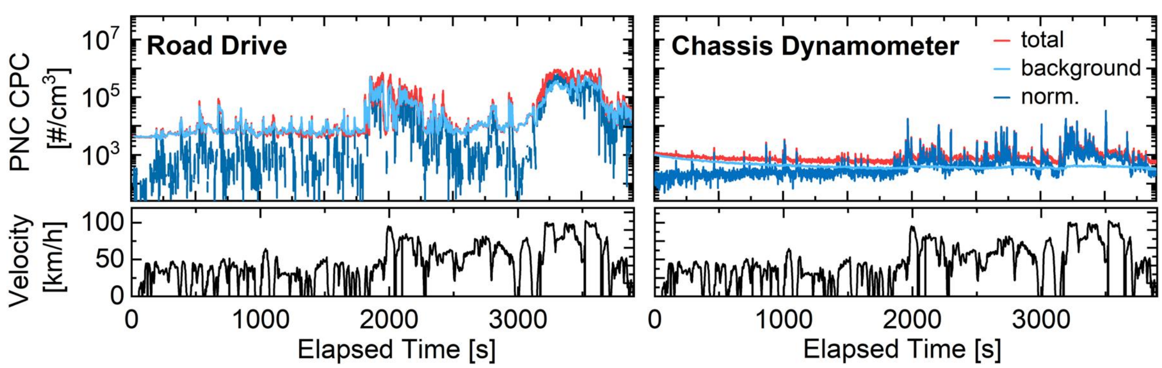

Figure 8. Comparison of TRWP emissions on the road (left) and on the chassis dynamometer (right) and the during a real driving emission test cycle.

number of all emitted particles, which is determined by the integral of all normalized emission curves, emissions are 12% lower on the dynamometer.

Also, there are differences in the size distribution as shown in Figure 5b. On the test track, additional UFP emissions of particles between 40 and 80 nm are measured, with a mode maximum at 60 nm. There are also differences in the weighting of the emission modes. While the 10 nm dominates by an order of magnitude on the chassis dynamometer, the 10 nm and 250 nm modes are at a similar level on the test track.

3.2.2. Cornering

Lateral forces have a significant influence on TRWP emissions, but cannot be investigated on the chassis dynamometer and were therefore part of the driving on the test track. Continuous cornering was tested in the narrow traffic circle (25 m diameter) at approximately 10, 20, and 30 km/h. Due to the tilted position of the on-board instrumentation, only EEPS data can be evaluated in this case. In Figure 6a the lower diagram shows the velocity and lateral acceleration of the vehicle in black and gray respectively. EEPS data is displayed in the middle and upper diagram, as total particle concentration and PSD. It should be noted that the EEPS data includes the background concentration on the test site. Nevertheless, a clear trend can be identified; particulate emissions increase with increasing velocity and increasing lateral acceleration from 1×10^4 #/cm^3 at 10 km/h, to 2×10^4 #/cm^3 at 20 km/h, to peak concentrations in the range of 10^5 #/cm^3 at 30 km/h. The emitted particle size is in similar as observed in the previous test; about 10, 60 and 270 nm.

Figure 6b shows the size distribution during the last section at 30 km/h in the traffic circle, as well as during braking and acceleration from Figure 7 (left-hand side). For both driving maneuvers, particles are emitted in three different size ranges, but the relative amount is significantly different. During cornering, all three size ranges are similar, whereas during acceleration and braking on a straight road, emissions are significantly lower at around 60 nm and fine particle emissions at 270 nm predominate.

3.2.3. Road drive

The experimental setup was also tested on real roads to cover all driving scenarios, such as high velocities and different road surfaces. Emission measurements at the tire housing during mobile on-road measurements are shown on the left side of Figure 8. The lower graph shows the vehicle velocity in black. The upper graph shows the CPC concentration during the primary sampling in light blue and the concentration normalized by the secondary sampling measurements in dark blue. While total emissions are very low during urban driving, there are extremely high values for both total particle number and normalized concentration at the beginning of interurban driving (1800s) and during highway driving (3200s). These high values are dominated by a single emission mode from 6 to 25 nm, with its maximum at 10 nm.

For comparison, the real drive was repeated on the dynamometer using the recorded velocity and grade, and the corresponding data is shown on the right in Figure 8. Road measurements result in a normalized PNC as high as 6×10^5 #/cm^3, whereas the normalized PNC on the dynamometer are more than an order of magnitude lower at 3×10^4 #/cm^3. There is a correlation between velocity and normalized PNC on the chassis dynamometer, which is not the case on the road. Both differences indicate that background normalization cannot be applied for road tests with traffic, which is presumably due to fluctuating- and high background concentrations. Consequently, the normalized PNC does probably not correspond to the real TRWP emissions for road driving.

4. Conclusion

A comprehensive study was conducted to measure and characterize the tire and road wear particle (TRWP) emissions from a new sampling system, revealing a bimodal size distribution with dominant ultrafine particles, and investigating various factors such as driving cycles, road surface, and lateral acceleration on TRWP emissions.

The presented on-vehicle measurement setup facilitates data interpretation by eliminating direct brake emissions due to the separate brake and tire enclosures. By additional measurement of the local background concentration of particles, it is possible to detect low concentrations of TRWP emissions and relate emissions to vehicle and driving parameters.

Due to the climatic chamber of the chassis dynamometer, background concentrations are well below typical ambient air values, allowing emissions to be normalized despite the open sampling system. The emitted particles show size ranges of 10 nm in the ultrafine range and 270 nm in the fine particle range which are in good agreement with the results of previous component and dynamometer tests. Airborne particle number concentration is mainly covered by the measurement range of the CPC (4 nm to 3 µm), as OPS measurements indicate low PNCs between 3 µm and 10 µm. SEM-EDX examinations show different particle types, which indicate different processes of particle formation. The chemical composition is dominated by carbon, oxygen and iron, with the latter presumably originating from the drum surface.

The measurement of different driving cycles and test profiles shows the large variance of the emission indices from 1.15×10^9 #/km for the LA4 to 2.75×10^9 #/km for the US06. This underscores the need to develop a representative driving cycle to study

TRWP emissions and the necessity of real-world driving emissions measurements.

Mobile measurements enable real-drive emission characterization. On the test track same driving behavior results in similar emission curves than on the chassis dynamometer. However, the level of fine and ultrafine particle emissions can vary. Comparing the emission size ranges for cornering and straight acceleration and deceleration on the test site indicates that lateral acceleration results in additional UFP emissions with a particle diameter of about 60 nm. The functionality of the test vehicle on a test track has been successfully demonstrated, yet a larger test site is required to quantify high velocity emissions.

For on-road tests, comparison with the dynamometer helps to validate the real driving emission measurements and also shows the limits of the sampling system. In the case of high and rapidly fluctuating background concentrations caused by other vehicles, mainly internal combustion engines, normalization by the second sampling of the background concentration is not possible with the system presented. Additional measurements in cleaner environments, on cleaner test grounds, and away from emissions from other traffic, would lead to further relevant results.

A comparison of the size distributions on the chassis dynamometer and on the test track shows similarities - such as the 10 nm mode - but also differences in emission behavior. The need for real measurements for the characterization of cornering is particularly significant, as there is a clear difference in the size distribution between straight and cornering on the test track, which indicates different formation processes. Consequently, the chassis dynamometer is a valuable tool for comparing the TRWP of different cycles or tires, but for a comprehensive characterization of emissions, additional mobile measurements on a test track are essential.

Acknowledgements

The authors acknowledge Ulrich Vogt and Miriam Chacón Mateos from the University of Stuttgart for supporting the measurements. In addition, the authors would like to thank Heribert Hellstern, Jens Kreeb, Marcel Frietsch, and Nina Gaiser from the German Aerospace Center for support during the measurement campaign.

Disclosure statement

No potential conflict of interest was reported by the author(s).

Funding

Funding of the project ZEDU-1 by the Ministry of Economy, Labor and Tourism Baden-Württemberg (Ministerium für Wirtschaft, Arbeit und Tourismus Baden-Württemberg) is gratefully acknowledged.

ORCID

Linda Bondorf http://orcid.org/0000-0001-5915-9233
Manuel Löber http://orcid.org/0000-0002-4492-952X
Tobias Grein http://orcid.org/0009-0006-0018-1915
Tobias Schripp http://orcid.org/0000-0002-1594-7331
Franz Philipps http://orcid.org/0009-0007-3569-3387

References

Alves, C. A., A. M. P. Vicente, A. I. Calvo, D. Baumgardner, F. Amato, X. Querol, C. Pio, and M. Gustafsson. 2020. Physical and chemical properties of non-exhaust particles generated from wear between pavements and tyres. *Atmos. Environ.* 224:117252. doi: 10.1016/j.atmosenv.2019.117252.

Aranke, O., W. Algenaid, S. Awe, and S. Joshi. 2019. Coatings for automotive gray cast iron brake discs: A review. *Coatings* 9 (9):552. doi: 10.3390/coatings9090552.

Beji, A., K. Deboudt, S. Khardi, B. Muresan, and L. Lumière. 2021. Determinants of rear-of-wheel and tire-road wear particle emissions by light-duty vehicles using on-road and test track experiments. *Atmos. Pollut. Res.* 12 (3):278–91. doi: 10.1016/j.apr.2020.12.014.

Bondorf, L., L. Köhler, T. Grein, F. Epple, F. Philipps, M. Aigner, and T. Schripp. 2023. Airborne brake wear emissions from a battery electric vehicle. *Atmosphere* 14 (3): 488. doi: 10.3390/atmos14030488.

Chang, X. D., H. B. Huang, R. N. Jiao, and J. P. Liu. 2020. Experimental investigation on the characteristics of tire wear particles under different non-vehicle operating parameters. *Tribol. Int.* 150 (10):106354. doi: 10.1016/j.triboint.2020.106354.

Charbouillot, T., D. C. Janet, P. Schaal, I. Beynier, J.-M. Boulat, A. Grandchamp, and F. Biesse. 2023. Methodology for the direct measurement of tire emission factors. *Sci. Total Environ.* 863:160853. doi: 10.1016/j.scitotenv.2022.160853.

Dahl, A., A. Gharibi, E. Swietlicki, A. Gudmundsson, M. Bohgard, A. Ljungman, G. Blomqvist, and M. Gustafsson. 2006. Traffic-generated emissions of ultrafine particles from pavement-tire interface. *Atmos. Environ.* 40 (7): 1314–23. doi: 10.1016/j.atmosenv.2005.10.029.

Dalmau, M. E., K. Augsburg, F. Wenzel, and V. Ivanov. 2020. Tire particle emissions: Demand on reliable characterization. *Tire Sci. Technol.* 48 (2):107–22. doi: 10.2346/tire.19.170181.

EU. 2024. Regulation (EU) 2024/1257 of the European Parliament and of the Council of 24 April 2024 on type-approval of motor vehicles and engines and of systems, components and separate technical units intended for such vehicles, with respect to their emissions and battery durability (Euro 7). *Off. J. Eur. Union.* 1257:1–49.

Feißel, T., M. Kunze, D. Hesse, V. Ivanov, K. Augsburg, and S. Gramstat. 2024. On-road vehicle measurement of tire wear particle emissions and approach for emission prediction. *Tire Sci. Technol.* 52 (1):2–14. doi: 10.2346/tire.22.21024.

Foitzik, M.-J., H.-J. Unrau, F. Gauterin, J. Dörnhöfer, and T. Koch. 2018. Investigation of ultra fine particulate matter emission of rubber tires. *Wear* 394-395:87–95. doi: 10.1016/j.wear.2017.09.023.

Fussell, J. C., M. Franklin, D. C. Green, M. Gustafsson, R. M. Harrison, W. Hicks, F. J. Kelly, F. Kishta, M. R. Miller, I. S. Mudway, et al. 2022. A review of road traffic-derived non-exhaust particles: Emissions, physicochemical characteristics, health risks, and mitigation measures. *Environ. Sci. Technol.* 56 (11):6813–35. doi: 10.1021/acs.est.2c01072.

Gehrke, I., S. Schläfle, R. Bertling, M. Öz, and K. Gregory. 2023. Review: Mitigation measures to reduce tire and road wear particles. *Sci. Total Environ.* 904:166537. doi: 10.1016/j.scitotenv.2023.166537.

GRBP-78-17, UNECE 2023. *Informal document GRBP-78-17: Vehicle method for measurement of tyre-to-road abrasion rate in real driving environment*. Geneva, Switzerland: United Nations Economic Commission for Europe (UNECE).

Grigoratos, T., M. Gustafsson, O. Eriksson, and G. Martini. 2018. Experimental investigation of tread wear and particle emission from tyres with different treadwear marking. *Atmos. Environ.* 182:200–12. doi: 10.1016/j.atmosenv.2018.03.049.

Hascoët, M., and L. Adamczak. 2020. At source brake dust collection system. *Results in Engineering* 5:100083. doi: 10.1016/j.rineng.2019.100083.

Jandacka, D., and D. Durcanska. 2019. Differentiation of particulate matter sources based on the chemical composition of PM10 in functional urban areas. *Atmosphere* 10 (10):583. doi: 10.3390/atmos10100583.

Johannessen, C., J. Liggio, X. Zhang, A. Saini, and T. Harner. 2022. Composition and transformation chemistry of tire-wear derived organic chemicals and implications for air pollution. *Atmos. Pollut. Res.* 13 (9):101533. doi: 10.1016/j.apr.2022.101533.

Kim, G., and S. Lee. 2018. Characteristics of tire wear particles generated by a tire simulator under various driving conditions. *Environ. Sci. Technol.* 52 (21):12153–61. doi: 10.1021/acs.est.8b03459.

Kumar, P., L. Pirjola, M. Ketzel, and R. M. Harrison. 2013. Nanoparticle emissions from 11 non-vehicle exhaust sources - A review. *Atmos. Environ.* 67:252–77. doi: 10.1016/j.atmosenv.2012.11.011.

Kwak, J. H., H. Kim, J. Lee, and S. Lee. 2013. Characterization of non-exhaust coarse and fine particles from on-road driving and laboratory measurements. *Sci. Total Environ.* 458-460:273–82. doi: 10.1016/j.scitotenv.2013.04.040.

Kwon, H. S., M. H. Ryu, and C. Carlsten. 2020. Ultrafine particles: Unique physicochemical properties relevant to health and disease. *Exp. Mol. Med.* 52 (3):318–28. doi: 10.1038/s12276-020-0405-1.

Lee, S., J. Kwak, H. Kim, and J. Lee. 2013. Properties of roadway particles from interaction between the tire and road pavement. *IntJ. Automot. Technol.* 14 (1):163–73. doi: 10.1007/s12239-013-0018-y.

Li, J., M. Zhang, Y. Ge, Y. Wen, J. Luo, D. Yin, C. Wang, and C. Wang. 2023. Emission characteristics of tyre wear particles from light-duty vehicles. *Atmosphere* 14 (4):724. doi: 10.3390/atmos14040724.

Lin, S., Y. Liu, H. Chen, S. Wu, V. Michalaki, P. Proctor, and G. Rowley. 2022. Impact of change in traffic flow on vehicle non-exhaust PM2.5 and PM10 emissions: A case study of the M25 motorway, UK. *Chemosphere* 303 (Pt 1):135069. doi: 10.1016/j.chemosphere.2022.135069.

Mathissen, M., V. Scheer, R. Vogt, and T. Benter. 2011. Investigation on the potential generation of ultrafine particles from the tire-road interface. *Atmos. Environ.* 45 (34):6172–9. doi: 10.1016/j.atmosenv.2011.08.032.

Park, I., H. Kim, and S. Lee. 2018. Characteristics of tire wear particles generated in a laboratory simulation of tire/road contact conditions. *J. Aerosol Sci.* 124:30–40. doi: 10.1016/j.jaerosci.2018.07.005.

Schläfle, S., H.-J. Unrau, and F. Gauterin. 2023. Influence of load condition, tire type, and ambient temperature on the emission of tire–road particulate matter. *Atmosphere* 14 (7):1095. doi: 10.3390/atmos14071095.

Schraufnagel, D. E. 2020. The health effects of ultrafine particles. *Exp. Mol. Med.* 52 (3):311–7. doi: 10.1038/s12276-020-0403-3.

Tonegawa, Y., and S. Sasaki. 2021. Development of tire-wear particle emission measurements for passenger vehicles. *Emiss. Control Sci. Technol.* 7 (1):56–62. doi: 10.1007/s40825-020-00181-z.

UN, ECE/TRANS/180/Add.24. 2023. UN global technical regulation No. 24: Laboratory measurement of brake emissions for light-duty vehicles.